Photodetachment of negative halogen ions

V. Radojević and H. P. Kelly
Department of Physics, University of Virginia, Charlottesville, Virginia 22901

W. R. Johnson
Department of Physics, University of Notre Dame, Notre Dame, Indiana 46556

(Received 15 October 1986)

Results of relativistic random-phase approximation calculations of photodetachment cross sections and angular-distribution asymmetry parameters are presented for the outer shells of the negative ions F^-, Cl^-, Br^-, and I^- in the photon-energy region from the threshold to about 100 eV. These results are compared with available theoretical calculations and with experimental data.

Measurements[1–7] and calculations[8–13] of photodetachment cross sections for negative halogen ions have all been restricted to energies less than 10 eV above threshold except for a recent many-body perturbation theory (MBPT) calculation[14] of Qian and Kelly for Cl^-. In view of the availability of experimental methods for extending the measurements to higher energies, we have undertaken calculations of the photodetachment parameters of F^-, Cl^-, Br^-, and I^- for energies from threshold up to about 100 eV above threshold, using the random-phase approximation (RPA).

The ground-state configuration of a negative halogen ion is the same as that of the corresponding noble gas, and therefore photodetachment of negative halogen ions is the same process as photoionization of noble-gas atoms. Since the RPA has been successful in explaining photoionization of noble-gas atoms,[15–17] it is of interest to study its applicability to systems such as negative ions, where electron-electron correlation is relatively more important. To account for the effects of the spin-orbit interaction automatically, we use the relativistic RPA (RRPA).[18,19]

In the present study only excitations of outermost subshells are considered (we use a truncated version of the RRPA), because the excitations of other, deeper subshells do not give any significant contribution to the photodetachment amplitudes in the region of energies studied. The amplitudes are calculated in the dipole approximation. As in the similar study of noble gases,[16,17] seven coupled channels are included for F^- ($n=2$) and Cl^- ($n=3$):

$$np_{3/2}\rightarrow d_{5/2},d_{3/2},s_{1/2}\ ,$$

$$np_{1/2}\rightarrow d_{3/2},s_{1/2}\ ,$$

$$ns_{1/2}\rightarrow p_{3/2},p_{1/2}\ ,$$

while in the cases of Br^- ($n=4$) and I^- ($n=5$) six more channels are added:

$$(n-1)d_{5/2}\rightarrow f_{7/2},f_{5/2},p_{3/2}\ ,$$

$$(n-1)d_{3/2}\rightarrow f_{5/2},p_{3/2},p_{1/2}\ .$$

The coupled RRPA equations are solved for the excited orbital in each channel and the resulting dipole amplitudes are evaluated using these excited orbitals.[18] The dipole amplitudes are then combined to determine the measurable photodetachment (photoionization) parameters.[16,17] Codes used previously to study the noble gases and other closed-shell atoms were modified to account for the non-Coulomb asymptotic behavior of the potential.

The theoretical threshold values in RPA calculations are the absolute values of the Hartree-Fock (HF) orbital eigenvalues [or in the case of the RRPA, Dirac-Hartree-Fock (DHF) eigenvalues]. These values are presented in Table I, where they are compared with the experimental data.

All the independent photoionization parameters—the

TABLE I. Photodetachment thresholds of halogen negative ions in eV. The calculated RRPA values (DHF energy eigenvalues) are compared with the experimental data. The experimental values for the first threshold (electron affinity) are taken from the recent review by Mead *et al.* (Ref. 20; also see Refs. 21 and 22); the experimental uncertainty of the last given digit is shown in parentheses after the value. The experimental values of the second threshold are obtained by adding the observed value of the splitting of the ^2P term (Ref. 23) to the value of the first threshold.

	$^2P_{3/2}$ threshold		$^2P_{1/2}$ threshold		$^2S_{1/2}$ threshold
Ion	RRPA	Expt.	RRPA	Expt.	RRPA
F^-	4.8886	3.399(3)	4.9684	3.448	29.335
Cl^-	4.0271	3.615(4)	4.1688	3.727	20.132
Br^-	3.5655	3.364(4)	4.1222	3.825	19.394
I^-	3.0893	3.0591(1)	4.2069	4.001	16.555

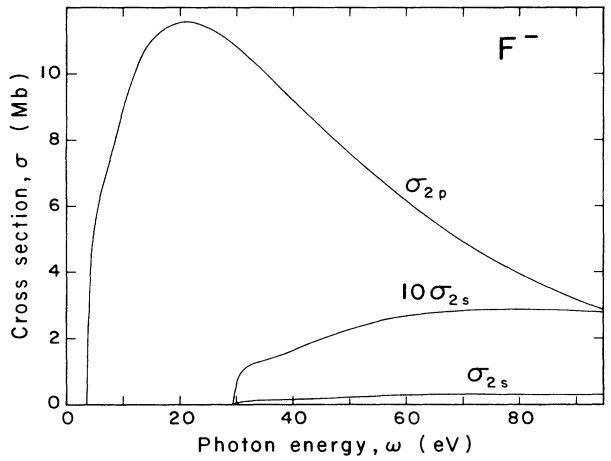

FIG. 1. RRPA partial photodetachment cross sections for the $2p$ and $2s$ shells of F^-.

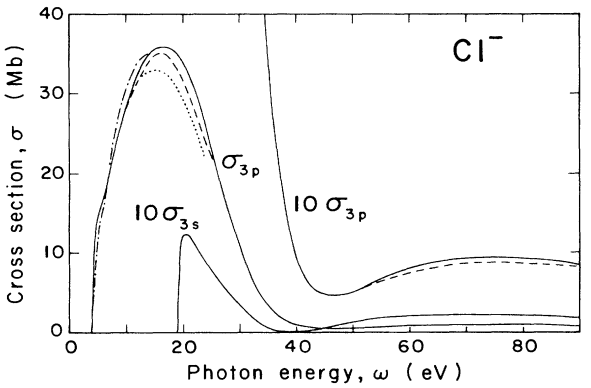

FIG. 2. Partial photodetachment cross sections for the $3p$ and $3s$ shells of Cl^-. ——, RRPA results; — — —, RRPA results in the velocity form, when different from the length form. MBPT result, in length form, —·—·—·, and velocity form, · · · · (Ref. 14).

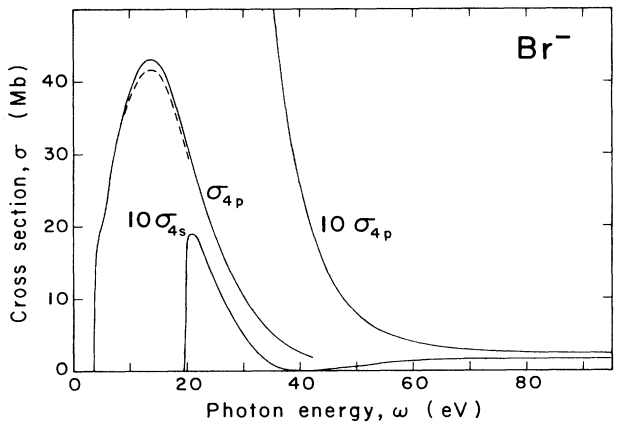

FIG. 3. Partial photodetachment cross sections for the $4p$ and $4s$ shells of Br^-. ——, RRPA results; — — —, RRPA results in the velocity form, when different from the length form.

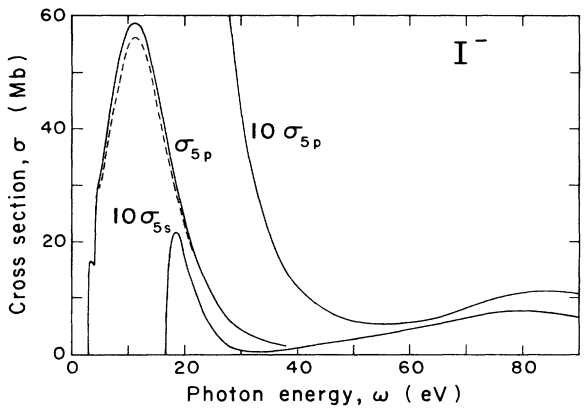

FIG. 4. Partial photodetachment cross sections for the $5p$ and $5s$ shells of I^-. ——, RRPA results; — — —, RRPA results in the velocity form, when different from the length form.

cross sections, branching ratios, photoelectron angular-distribution asymmetry parameters, and spin-polarization parameters—were calculated, although only some of these parameters are presented in the present article.

The results of our calculations for the cross section are shown in Figs. 1—4 for the entire region of energy considered. One sees from Fig. 2 that for Cl^- the results of our calculations agree well with the MBPT.[14] The overall shapes of the cross section curves are similar to the shapes of cross section curves for the corresponding noble-gas atoms,[15–17] except close to the thresholds. This difference in curve shapes close to the thresholds arises because the thresholds of halogen negative ions occur at much lower energies than the corresponding thresholds of noble gasses, and because partial cross sections near the threshold satisfy the Wigner law[24] and vanish at threshold. The Wigner law, which is a consequence of the non-

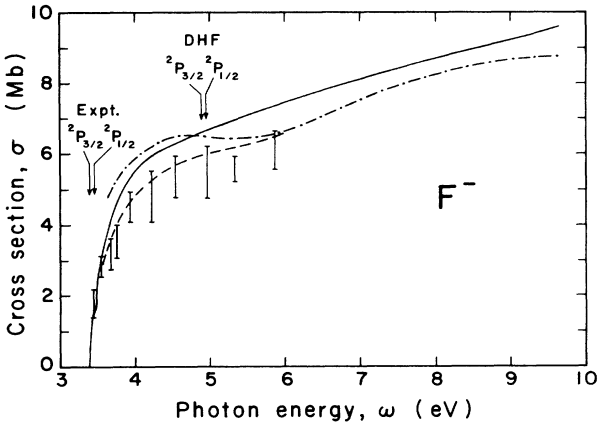

FIG. 5. The photodetachment cross section for F^- in the energy region close to the threshold. The RRPA results, ——, are compared with the experimental data from Ref. 3, I , with MBPT calculations by Foster and Ishihara, Ref. 13, — — —, and also with the Stieltjes imaging calculations by Rescigno *et al.*, Ref. 12, —·—·—·. The curve representing RRPA results is shifted from the theoretical threshold to the experimental one.

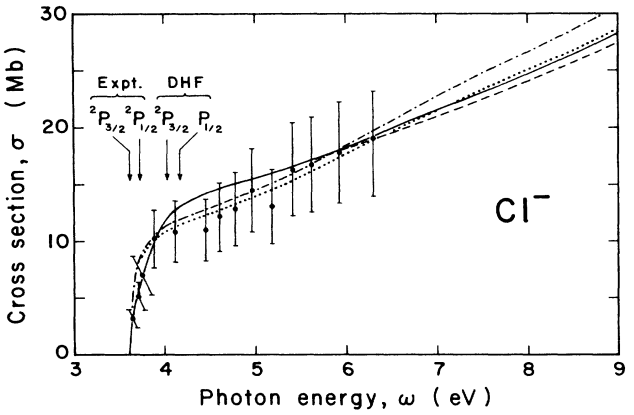

FIG. 6. The photodetachment cross section for Cl^- in the energy region close to the threshold. The RRPA results, —— (— — — results in the velocity form, when different from the length form), are compared with the experimental data of Ref. 6, ⌶, and with the MBPT calculations by Quian and Kelly, —·—·—· (length) and · · · · (velocity). The curves representing theoretical results (RRPA and MBPT) are shifted from their respective theoretical thresholds to the experimental ones.

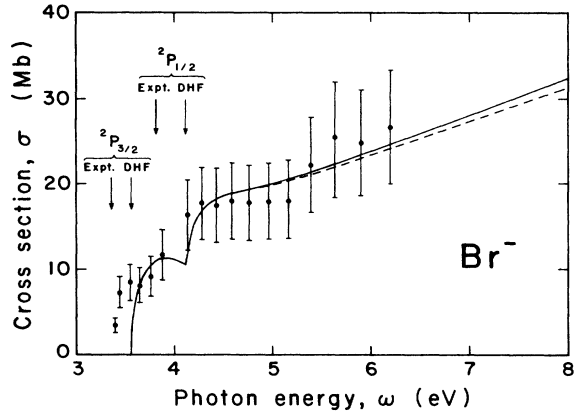

FIG. 7. The photodetachment cross section for Br^- in the energy region close to the threshold. The RRPA results, —— (— — — results in the velocity form, when different from the length form), are compared with the experimental data of Ref. 6, ⌶.

Coulombic asymptotic behavior of the atomic potential for negative ions, has the form

$$\sigma(k) = \text{const} \times k^{2l+1}[1+O(k^2)] ,$$

where $\sigma(k)$ is the cross section, k is the linear momentum of the photoelectron, and l is its orbital-angular-momentum quantum number. We find that the discrepancy between the length and velocity form results from our calculations is generally somewhat larger than the corresponding discrepancy for the noble gases.[16] This larger discrepancy is attributed to the increased importance of electron-electron interactions for the negative ions.

Because experimental results and other calculations are available only in the relatively small region of energies close to the threshold, we present in Figs. 5—8 the results of our calculations for cross sections in this region and make comparisons with experimental data and with other calculations. As seen from these figures, the overall agreement of our results with experimental data is quite reasonable. The theoretical MBPT results for F^- by Ishihara and Foster[13] seems to agree with the experimental data[3] somewhat better than our RRPA results, in spite of the fact that their MBPT results contain only first-order contributions which are also included in the RRPA. For all negative halogen ions, there exist older semiempirical model potential calculations by Robinson and Geltman[11] (claimed to have accuracy of ±20%) as well as similar calculations from Refs. 8—10. Although none of these potential theory results are presented here, they agree qualitatively with our results and with experimental data. The flat portion of the cross section curve for I^- between the $5p_{1/2}$ and $5p_{3/2}$ thresholds shown in Fig. 8 agrees better with these semiempirical calculations than with the experimental data, leading us to believe that the measured values in this region may possibly be too large.

Even though there are no experimental data on photodetachment parameters other than cross sections, we present results of RRPA calculations for the angular distribution asymmetry parameters β, hoping that such results will attract interest in the experimental determination of these parameters. In Figs. 9—12 are shown our results for the asymmetry parameter β_{np} of np shells. For F^- (Fig. 9), Cl^- (Fig. 10), and Br^- (Fig. 11) the values of the asymmetry parameters for the $np_{1/2}$ and $np_{3/2}$ subshells are found to be nearly identical, so only the average values

$$\beta_{np} = \frac{\beta_{np_{1/2}}\sigma_{np_{1/2}} + \beta_{np_{3/2}}\sigma_{np_{3/2}}}{\sigma_{np_{1/2}} + \sigma_{np_{3/2}}}$$

are shown. For I^- our results for the asymmetry parameters of the $5p_{1/2}$ and $5p_{3/2}$ subshells are not as close as

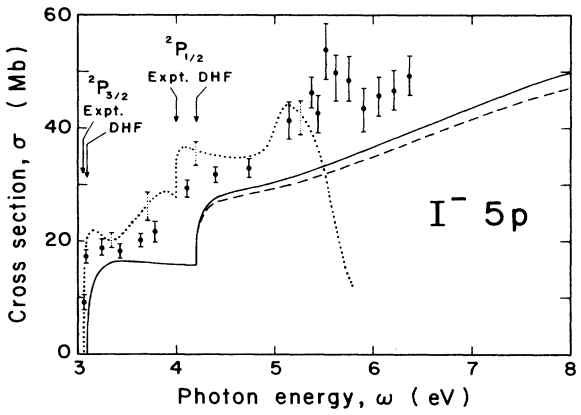

FIG. 8. The photodetachment cross section for I^- in the energy region close to the threshold. The RRPA results, —— (— — — results in the velocity form, when different from the length form), are compared with the experimental data of Refs. 4 (⌶) and 5 (· · · ·).

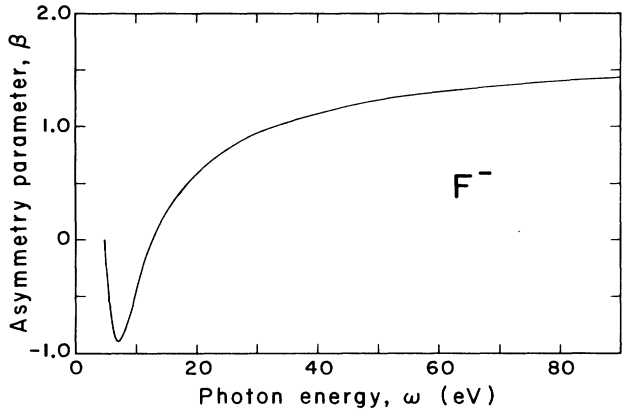

FIG. 9. RRPA results for the angular distribution asymmetry parameter of the $2p$ shell for F^-.

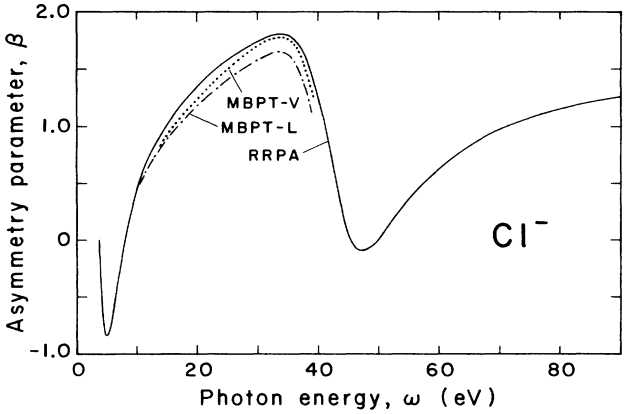

FIG. 10. RRPA values for the photoelectron angular distribution asymmetry parameter of the $3p$ shell of Cl^-. The RRPA results are compared with the recent MBPT values of Ref. 14, —·—·— (length) and · · · · (velocity).

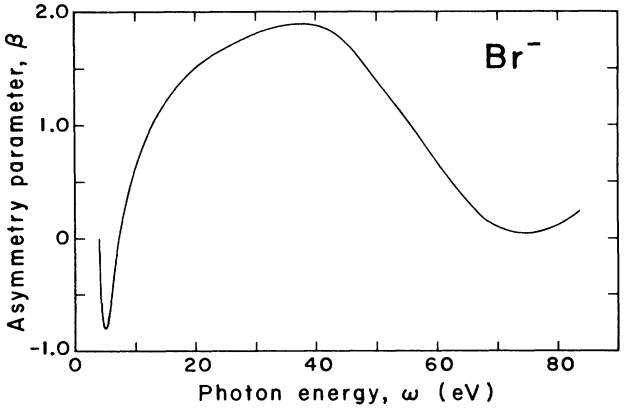

FIG. 11. RRPA results for the angular distribution asymmetry parameter of the $4p$ shell for Br^-.

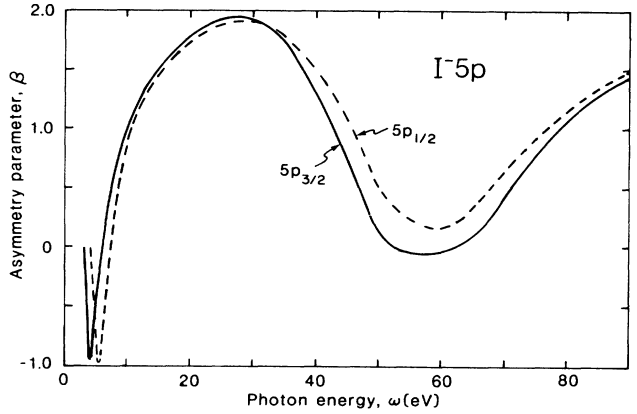

FIG. 12. RRPA results for the photoelectron angular distribution asymmetry parameters of the $5p_{1/2}$ and $5p_{3/2}$ subshells of I^-.

those for the lighter halogen atoms, so the subshell values are shown separately in Fig. 12. The shapes of the curves for the asymmetry parameter are, as for the cross sections, similar to the corresponding curves for noble-gas atoms,[16,17] except in the region close to the threshold, where the curves for all ions show a distinct minimum. In the figures we have presented only the length form for the parameter β_{np}; the length and velocity forms are found to be identical for all the cases studied on the scale of the figures. Because of the lack of other data for the parameter β_{np}, we only compare in Fig. 6 our results for Cl^- with the MBPT calculations of Ref. 14. As seen from the figure, our result practically coincides with the MBPT in the energy region up to 10 eV and agrees well for higher energies.

As discussed earlier,[16] the angular distribution parameter β_{ns} for the ns shell departs from its nonrelativistic

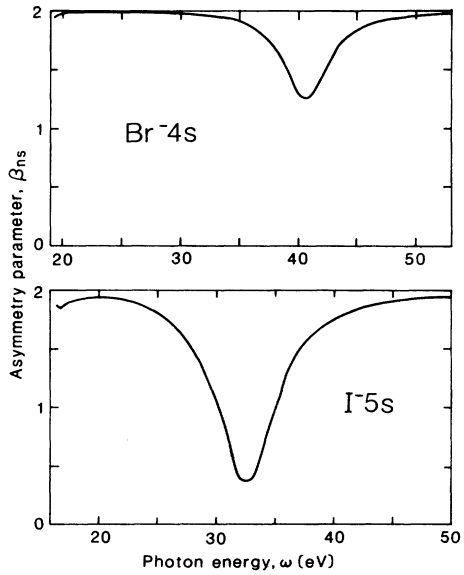

FIG. 13. RRPA results for the angular distribution asymmetry parameters β_{4s} of Br^- and β_{5s} of I^-.

constant value of 2 whenever the amplitude of the excited triplet state is not small compared to the amplitude of the excited singlet state. This can occur near the Cooper minimum, where the singlet amplitude is small. Since the relativistic effect on β_{ns} is noticeable only for Br^- and I^-, the RRPA results are presented for only these ions in Fig. 13. One might expect that some departure of β_{ns} from 2 would be seen close to the *ns* threshold where, according to the Wigner law,[24] the cross section vanishes. However, such an affect is barely observable in Fig. 13.

Our calculations indicate that one can apply the RRPA to negative ions, where the electron-electron interaction is expected to be more important than for neutral atoms or positive ions. Although there is a limited amount of experimental data available, the agreement of the RRPA calculations with these data is quite reasonable. The discrepancy between length and velocity form results for the cross sections is sometimes somewhat worse than for the corresponding neutral atoms, owing to the absence of Coulombic asymptotic behavior for the atomic core potential. It is interesting to note that the agreement between length and velocity form results for the asymmetry and spin-polarization parameters is better than that for the cross sections. This may perhaps be because the asymmetry and spin-polarization parameters are ratios of bilinear functions of the dipole amplitudes, while the cross sections are quadratic functions of the amplitudes, so that there appears to be a scaling between the amplitudes in length and velocity forms in the *truncated* RRPA. The shapes of the curves for the RRPA photodetachment parameters are similar to the shapes for the corresponding noble-gas atoms, except in the vicinity of the thresholds, where non-Coulombic behavior of the atomic core potential comes into play. The experimental data exist only for cross sections in the energy region close to the first threshold, and the agreement of our calculation with experimental data is comparable to the agreement of the MBPT calculations. It would be desirable to have experimental data for photodetachment parameters other than cross sections, and to have the experimental data in a larger energy region.

ACKNOWLEDGMENTS

The work of two of us (V.R. and H.P.K.) was supported in part by the National Science Foundation Grant No. PHY-83-04239, while that of W.R.J. was supported in part by NSF Grant No. PHY83-08136. V.R. would like to acknowledge a computational grant from the Academic Computing Center of the University of Virginia.

[1]B. Steiner, Phys. Rev. **173**, 136 (1968).
[2]D. E. Rothe, Phys. Rev. **177**, 93 (1969).
[3]A. Mandl, Phys. Rev. A **3**, 251 (1971).
[4]A. Mandl and H. A. Hyman, Phys. Rev. Lett. **31**, 417 (1973).
[5]M. Neiger, Z. Naturforsch. **30A**, 474 (1975).
[6]A. Mandl, Phys. Rev. A **14**, 345 (1976).
[7]Earlier experimental results can be found in Refs. 1–6.
[8]J. W. Cooper and J. B. Martin, Phys. Rev. **126**, 1482 (1962).
[9]Y. V. Moskvin, Opt. Spektrosk. **17**, 499 (1964) [Opt. Spectrosc. (USSR) **17**, 270 (1964)].
[10]Y. V. Moskvin, Teplofiz. Vys. Temp. **3**, 821 (1965) [High Temp. (USSR) **3**, 765 (1965)].
[11]E. J. Robinson and S. Geltman, Phys. Rev. **153**, 4 (1967).
[12]T. N. Rescigno, C. F. Bender, and V. B. McKoy, Phys. Rev. A **17**, 645 (1978).
[13]T. Ishihara and T. C. Foster, Phys. Rev. A **9**, 2350 (1974).
[14]Z.-D. Qian and H. P. Kelly (unpublished).
[15]M. Ya. Amusia and N. A. Cherepkov, Case Study At. Phys. **5**, 47 (1975).
[16]W. R. Johnson and K. T. Cheng, Phys. Rev. A **20**, 978 (1979).
[17]K.-N. Huang, W. R. Johnson, and K. T. Cheng, At. Data Nucl. Data Tables **26**, 33 (1981).
[18]W. R. Johnson and C. D. Lin, Phys. Rev. A **20**, 964 (1979).
[19]W. R. Johnson, C. D. Lin, K. T. Cheng, and C. M. Lee, Phys. Scr. **21**, 409 (1980).
[20]R. D. Mead, A. E. Stevens, and W. C. Lineberger, in *Gas Phase Ion Chemistry,* edited by M. T. Bowers (Academic, New York, 1984), Vol. 3, Chap. 22, pp. 213–248.
[21]A. A. Radzig and B. M. Smirnov, *Reference Data on Atoms, Molecules, and Ions* (Springer-Verlag, Berlin 1985).
[22]B. M. Smirnov, *Negative Ions* (McGraw-Hill, New York, 1982).
[23]C. E. Moore, *Atomic Energy Levels,* Natl. Bur. Stand. (U.S.) Circ. No. 467 (U.S. GPO, Washington, D. C., 1971), Vols. I–III.
[24]E. P. Wigner, Phys. Rev. **73**, 1002 (1948).